THE JOURNAL OF PHYSICAL CHEMISTRY A

Article

pubs.acs.org/JPCA

Chiroptical Inversion Induced by Rotation of a Carbon−Carbon Single Bond: An Experimental and Theoretical Study

Wei Lu, Ganhong Du, Keyuan Liu, Liming Jiang,* Jun Ling,* and Zhiquan Shen

MOE Key Laboratory of Macromolecular Synthesis and Functionalization, Department of Polymer Science and Engineering, Zhejiang University, Hangzhou 310027, China

Supporting Information

ABSTRACT: We propose a new strategy to construct chiral molecular switches with highly reversible and sensitive chiroptical responses to variations in the external environment. Its fundamental concept involves a stimuli-triggered exchange of two conformations presenting significantly different chiroptical properties through the rotation of a carbon−carbon single bond, as demonstrated by chiral Schiff bases *s*-**1**, *s*-**2**, and a salicylamide analogue *s*-**3**. Upon addition of base in solution, the circular dichroism (CD) spectra of these molecular switches displayed unique changes featuring an inversion of the Cotton effect's signs, and the original CD profiles can be recoverd by acidification. Various spectroscopic studies as well as the conformational analysis combining with TDDFT computations allowed clear elucidation of the chiroptical inversion mechanism. It is expected that this kind of chiroptical switches is of great interest for molecular recognition, chemosensing, and the construction of molecular-scale devices. Furthermore, the present study indicates that the use of the conformational transition about a single bond may serve as the basis for designing chiroptical inversion systems.

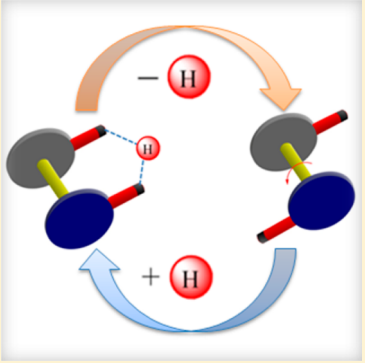

INTRODUCTION

Chiral and helical inversion phenomena are very common signal transfers and molecular motions in natural living organisms. External stimulus-responsive inversions of chiroptical properties are found to be important in many biological processes, including DNA and gene-involved functional expressions.[1,2] A drastic change in chiroptical properties makes dynamic chiroptical inversion systems especially suitable for use in chemosensing[3] as well as in molecular-level devices such as molecular switches and molecular motors.[4−8]

Chiroptical inversion usually involves cleavage of a noncovalent bond or weak interaction followed by rearrangement to another optically pure diastereomer.[9] For example, a lot of chiral supramolecular aggregates,[10−14] polymers,[15−35] foldamers,[36−46] and metal complexes[47−64] have been shown to offer helicity inversion induced by external stimuli, because in these systems the hydrogen-bonding, $\pi-\pi$ stacking, or metal coordination does not have enough strength to fix the single-handed helical or folded structures.

For certain chiral molecular switches based on the sterically overcrowded olefins, diarylethenes, and helicenes, the reversible and stereochemically controlled transformation of one optically pure diastereomer to another is realized through the cleavage and formation of a π-bond, and even of σ-bond.[26,65−73] The lifetime of these molecular switches is frequently short. Their inherent drawback stems from the well-known fact that no chemical reaction can proceed with 100% conversion.[9]

The chiroptical switches based on a single bond movement appear to be particularly attractive, because the molecular conformation states are highly sensitive to changes in the external environment, which is one feature desirable for many applications. In fact, there have been recently a few reports about molecular switches capable of producing chiroptical inversion due to the rotation of a single bond induced by solvent or metal coordination.[74−76] However, these systems are structurally complex and there is limited space for further molecular design.

Herein we describe a new approach to construct chiral molecular switches with the features of stimuli-controlled and reversible chiroptical inversion. Its fundamental concept involves an interchange of two conformations presenting diverse chiroptical properties by acid/base-mediated C−C single bond rotation. As a proof of principle, a simple chiroptical molecular switch has been established using *N*-salicylidene Schiff base of chiral α-phenylethylamine (*s*-**1**) as a peculiar skeleton motif (Scheme 1), which shows unique chiroptical responses in different pH environments. To prove the general applicability of the present strategy, we also synthesized 2-hydroxyl-1-naphthaldehyde Schiff base derivative *s*-**2** and salicylamide analog *s*-**3**. The results showed that the chiroptical properties of these compounds can be reversibly modulated after sequential reactions with base and acid, and thus a chiroptical molecular switch with nondestructive output signal is realized. On the basis of the combined use of spectroscopic measurement, conformational analysis, and time-dependent density functional theory (TDDFT) computation,

Received: October 20, 2013
Revised: December 2, 2013
Published: December 16, 2013

   dx.doi.org/10.1021/jp410370q | *J. Phys. Chem. A* 2014, 118, 283−292

Scheme 1. Structures of Schiff Bases (*s*-1 and *s*-2, Including the Enol and Keto Forms) and (*S*)-Salicylamide (*s*-3) as Well as Their Deprotonated Species

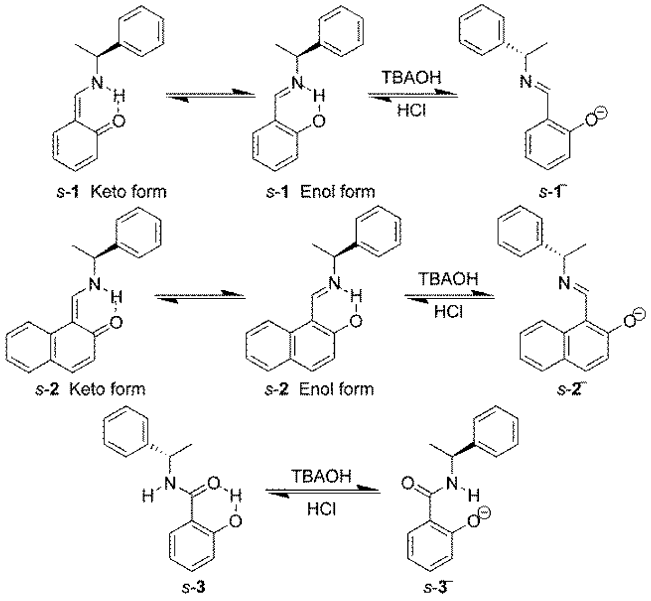

the working mechanism of chiroptical inversion is discussed in detail.

RESULTS AND DISCUSSION

Schiff Base Chiroptical Molecular Switch. Chiral *N*-salicylidene Schiff base (*s*-**1** or *r*-**1**) was straightforwardly synthesized by the condensation reaction of salicylaldehyde with optically pure α-phenylethylamine. The structural characterization data are provided in the Supporting Information. On the basis of well-established stereochemistry of *N*-salicylidene derivatives of chiral amines,[77,78] it is anticipated that the chiral compound would display evident CD signals due to the electric dipole−dipole coupling interaction of the salicylidenamino chromophore and the phenyl group in the chiral unit. In view of the strong dependency of keto−enol tautomerism on solvent nature, the optical properties of *s*-**1** were first examined by absorption and CD spectrocopies in various media (Figure 1).

As shown in Figure 1, two intensive positive CD signals near 316 nm (band I) and 252 nm (band II) are observed in DMSO, THF, DCM, or *n*-hexane, which correspond to the UV−vis absorption attributed to the $\pi-\pi^*$ transition of the intramolecularly hydrogen-bonded salicylidenamino chromophore in the enol form (Scheme 1). For the ethanol solution of *s*-**1**, a weak CD band in the range of 375−425 nm appears in addition to bands I and II. This characteristic signal is believed to arise from its keto form. According to ^{13}C NMR analysis, *s*-**1** exists only in the enol form in DMSO.[79,80] It should be noted that the 316 and 252 nm CD bands are both positive with no sign of exciton splitting. Similar phenomena were previously observed by H. E. Smith and considered to be related to the configuration interaction or weak exciton coupling as a result of vibrational effect cannot be ruled out.[77]

The change in CD and UV−vis spectra of *s*-**1** upon successive addition of tetrabutylammonium hydroxide (TBAOH) was recorded in DMSO for the purpose of removing interference from the keto tautomer. Upon titration of *s*-**1** with OH^-, the absorption maximum at 316 nm gradually

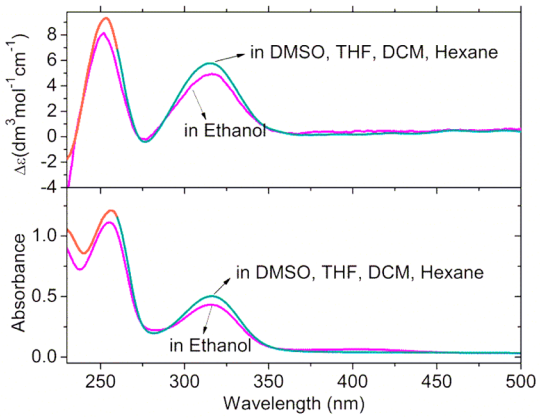

Figure 1. CD and UV−vis spectra of *s*-**1** (1×10^{-4} mol/L) in various solvents at ambient temperature (DMSO, dimethyl sulfoxide; THF, tetrahydrofuran; DCM, dichloromethane).

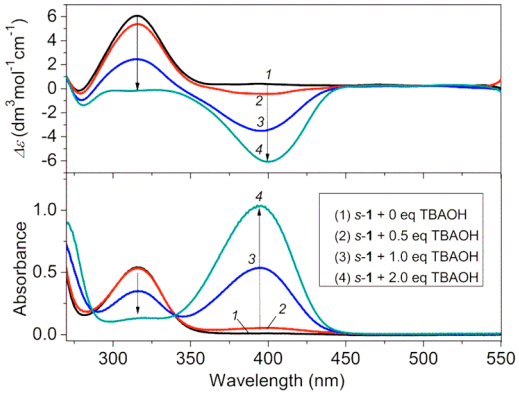

Figure 2. CD and UV−vis titration spectra of *s*-**1** (1×10^{-4} mol/L) in DMSO with increasing amount of TBAOH (0, 0.5, 1.0, and 2.0 equiv, respectively).

disappeared and a new band around 400 nm concomitantly appeared (Figure 2) due to the formation of deprotonated species *s*-**1**$^-$. The presence of a sharp isosbestic point at 340 nm indicates that only two species coexists in the equilibrium over the course of titration. Of great interest is that a complete inversion of the Cotton effect (CE) occurred with a red shift of ~80 nm when ~2 equiv of TBAOH was added, although the CD profiles of *s*-**1** and *s*-**1**$^-$ are not mirror images of each other.

It is worth mentioning that such a chiroptical response is completely reversible for the molecular switch. The CD spectral changes of *s*-**1** remain consistent after many deprotonation/protonation cycles without a distinct decay in the signal intensity, proving robust reversibility of this kind of chiroptical molecular switch (Figure S1, Supporting Information). Meanwhile, its optical rotation values in solution could be also reversibly tuned through cyclical addition of base and acid and is accompanied by reversible inversion of the optical rotation direction. As expected, the enantiomer of *s*-**1** exhibited the identical chiroptical inversion behavior (Figure S2, Supporting Information).

A series of control experiments confirmed that the observed chiroptical inversion for *s*-**1** is hardly affected by different kinds of base, counterion and solvent, although there exists a small difference in the magnitude (see Figures S3−S5 in the Supporting Information for details). Therefore, it is reasonable

dx.doi.org/10.1021/jp410370q | J. Phys. Chem. A 2014, 118, 283−292

to speculate that the chiroptical switch triggered by acid/base should work at a single-molecule level as a result of the changes in the electronic and conformational states of the interacting chromophores rather than the structure of a certain chiral supramolecular assembly.

To gain insight into the chiroptical switching mechanism of *s*-**1**, we performed the electronic circular dichroism (ECD) calculations with the aid of time-dependent density functional theory (TDDFT). Because CD spectroscopy is quite sensitive to slight changes in the geometry and electronic displacement of given chemical species, the combination of experimental and theoretical CD data would possibly allow one to elucidate the origin of observed chiroptical properties for the molecular switch. In fact, this method has proved to be effective and reliable for configurational and conformational analysis of organic compounds.[81−91]

The B3LYP functional and the 6-311++G** basis set were first used for geometry optimizations in vacuum. The computed structures for the three energy miminum conformers of *s*-**1** (denoted as *s*-**1a**∼**c**) are shown in Figure S6 (Supporting Information). Among them, the conformer *s*-**1c** is preferred over *s*-**1a** and *s*-**1b** by 2.25 and 1.41 kcal/mol, respectively. The computed conformer of lowest energy is in good agreement with the known single-crystal X-ray diffraction structure (Figure 3)[92] and Smith's conformational analysis as well.[77]

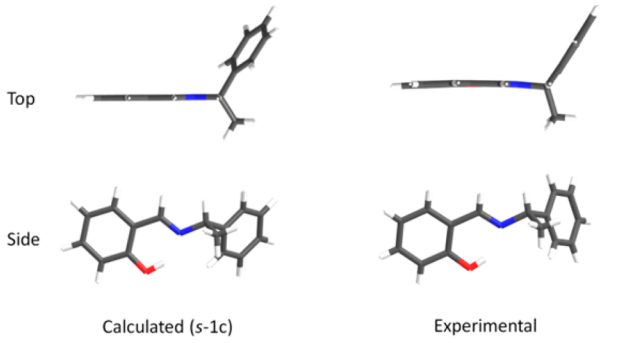

Figure 3. Comparison of (left) the computed structure for the most stable conformer *s*-**1c** in vacuum obtained at the B3LYP/6-311++G** level of theory and (right) the reported single-crystal structure of *s*-**1** from ref 92.

We then carried out the geometry optimizations of *s*-**1** with the PCM solvent model for DMSO in which the experimental CD data are collected. As shown in Figure 4, the three most stable conformers suggested by the solvent model have the same structure as those optimized in vacumm. All the conformers are stabilized by a strong intramolecular hydrogen bond between the phenolic hydrogen and the imine residue; their relative energies, Boltzmann weights, and selected hydrogen-bonded parameters are listed in Table 1. The lowest-energy conformer *s*-**1c** has a Boltzmann weight of 91.92% owing to its less steric hindrance, which is preferred over *s*-**1a** (3.18%) and *s*-**1b** (4.90%) by 1.99 and 1.74 kcal/mol, respectively. Moreover, the fact that the stability of conformer *s*-**1b** is slightly greater than *s*-**1a** could be attributed to the intramolecular C—H···π interaction between −N═C—H and the phenyl group attached to the chiral center in the former. Thus, TDDFT calculations on the three preferred conformers followed by Boltzmann weighting resulted in an average ECD spectrum in well consistent with the experimental except that the position of the predicted Cotton effect is at a shorter wavelength (306 nm) than the measured value (316 nm) (Figure 5a). As for the deprotonated *s*-**1**, TDDFT calculations reveal that only one dominant conformer, i.e., *s*-**1d** was identified in the conformational searches with a 10 kcal/mol energy window. This result seems to be reasonable because the conformer adopts the least sterically hindered arrangement compared with other possible isomers resulting from rotation about the chiral carbon−nitrogen single bond. Similarly, there is a good agreement between the theoretical ECD curve and the experimental spectrum in DMSO for *s*-**1**$^-$, wherein the

Table 1. Relative Energies (ΔE_0, kcal/mol), Boltzmann Weights (BW, 298 K), and Intramolecular Distances C−H···π ($d_{C-H\cdots\pi}$, Å) and O−H···N ($r_{O-H\cdots N}$, Å)

conformer	ΔE_0 (kcal/mol)	BW (%)	$d_{C-H\cdots\pi}$ (Å)[a]	$r_{O-H\cdots N}$ (Å)[b]
s-**1a**	1.99	3.18		1.704
s-**1b**	1.74	4.90	2.494	1.708
s-**1c**	0.00	91.92		1.724

[a] $d_{C-H\cdots\pi}$ is the distance between methine hydrogen of salicylidene and the carbon of the phenyl group directly attached to the chiral center. [b] $r_{O-H\cdots N}$ is the distance between the hydrogen of phenolic hydroxyl group and the imine nitrogen.

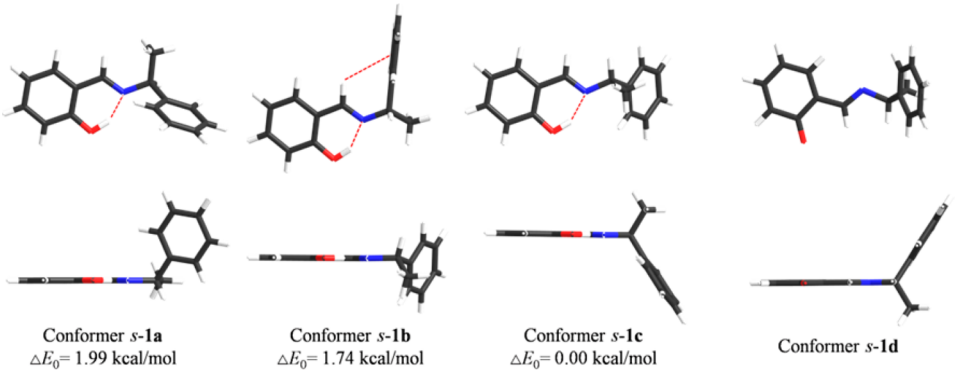

Figure 4. Computed structures of most stable conformers for *s*-**1** (*s*-**1a**−**c**) and the dominant conformer for *s*-**1**$^-$ (*s*-**1d**) obtained at the B3LYP/6-311++G**/IEFPCM (DMSO) level of theory (with relative energies). Each conformer is shown as a side (above) and top (below) view. Note: oxygen and nitrogen atoms are red and blue, respectively; the intramolecular hydrogen bond or C−H···π interaction is represented in a red dotted line for clarity.

dx.doi.org/10.1021/jp410370q | J. Phys. Chem. A 2014, 118, 283−292

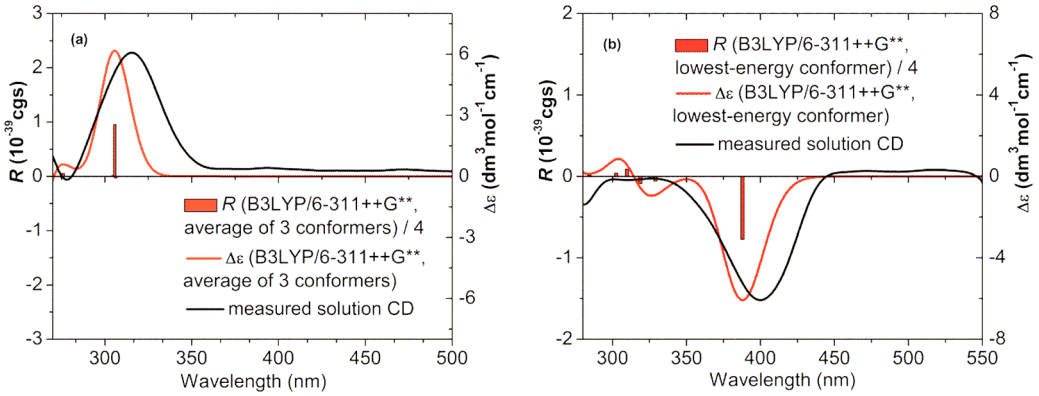

Figure 5. Comparison of the calculated (B3LYP/6-311++G**/IEFPCM(DMSO), red line) and experimental (black line) ECD spectra in DMSO for *s*-**1** (a) and *s*-**1**$^-$ (b). Vertical bars represent the rotational strengths **R** in 10^{-39} cgs units.

former displays a strong negative Cotton effect near 388 nm (Figure 5b). These observations indicate that the TDDFT functional with the IEFPCM solvent model proves to be an effective and reliable method for ECD calculations in the present study.

On the basis of the above-mentioned facts, it is clear that the conformers *s*-**1c** and *s*-**1d** are the most important contributors to the dichroic absorption of free *s*-**1** and its deprotonated species, respectively. Between the two preferred conformers there exists a distinct difference in the spatial arrangement of groups at the chiral center with respect to the salicylidenamino chromophore. Nevertheless, they can interconvert from one to another by a 180°-rotation of the C−C bond connecting the azomethine to phenyl group in the salicylidene moiety under the stimulus of acid/base, as depicted in Figure 6. That is, the

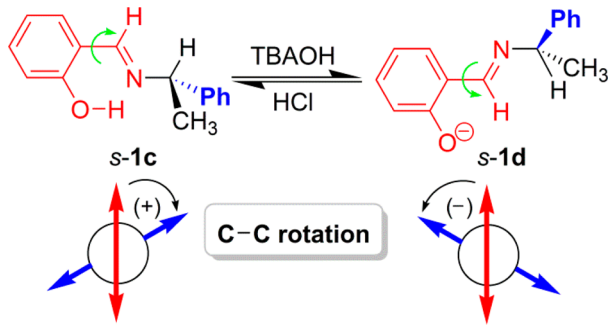

Figure 6. Prediction of CD signs for *s*-**1** and *s*-**1**$^-$ on the basis of their respective preferred conformations (*s*-**1c**, *s*-**1d**) obtained at the B3LYP/6-311++G**/IEFPCM(DMSO) level of theory. Each conformer has a particular chirality of coupling as shown.

deprotonation/protonation of the phenolic hydroxy group and accompanying conformational transition about the C−C bond are responsible for the chiroptical inversion of the Schiff base molecular switch. Furthermore, such a chiroptical inversion may be interpreted in terms of the exciton chirality rule.[93] From the known transition moment directions of the two intramolecularly interacting chromophores,[77,78] we can predict that the most stable conformer *s*-**1c** makes a negative contribution to the CE near 316 nm, whereas the contribution of *s*-**1d** is negative to the 400 nm CE for the deprotonated species *s*-**1**$^-$ (Figure 6).

2-Hydroxyl-1-naphthaldehyde Schiff base of (*S*)-*α*-phenylethylamine *s*-**2** and its ethylated derivative Et-*s*-**2** provide a remarkable example to further account for the above-proposed chiroptical inversion mechanism. As anticipated, *s*-**2** was found to display the base/acid induced chiroptical response similar to that of *s*-**1** (Figure S8, Supporting Information). More interestingly, the observed CD spectra appear to give a quasi-mirror image for *s*-**2** vs Et-*s*-**2** as shown in Figure 7.[94] At the same time, TDDFT calculations revealed that the geometry-optimized conformation of Et-*s*-**2** is quite close to the most

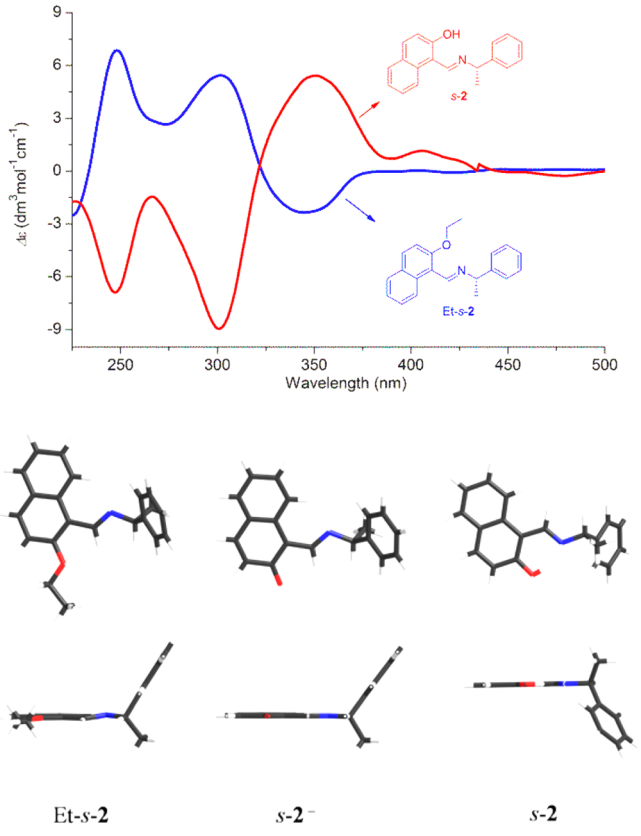

Figure 7. Top: CD spectra of *s*-**2** and Et-*s*-**2** (1×10^{-4} mol/L) in *n*-hexane/THF (4:1, v/v) solution. Notice that in the mixed solvent *s*-**2** exists dominantly in the enol form estimated by UV−vis spectra (Figure S7, Supporting Information). Bottom: optimized structures of the most stable conformers of Et-*s*-**2**, *s*-**2**, and *s*-**2**$^-$ obtained at the B3LYP/6-311++G**/IEFPCM(DMSO) level of theory, in which oxygen and nitrogen atoms are red and blue, respectively. Each conformer is shown as a side (above) and top (below) view.

dx.doi.org/10.1021/jp410370q | J. Phys. Chem. A 2014, 118, 283−292

stable conformer of the deprotonated *s*-**2**.[95] In other words, Et-*s*-**2** takes a conformation in which the ethoxyl group is far away from the imine nitrogen atom just as does the naphtholate oxyanion in *s*-**2**$^-$ via the naphthyl group rotation about its attachment bond. In addition, the theoretical ECD spectra are in a good agreement with the main bands of the corresponding experiment for the *N*-*α*-naphthal derivatives (Figures S9−S11, Supporting Information).

Amide Chiroptical Molecular Switch. With the chiroptical inversion mechanism of the salicylaldehyde Schiff in mind, we further investigated the chiroptical properties of salicylamide of (*S*)-*α*-phenylethylamine (*s*-**3**) to examine whether the above observation has general applicability. Choosing salicylamide derivative is mainly owing to the following two reasons. First, the intramolecularly hydrogen-bonded salicylamide moiety is structurally similar to the salicylidenamino chromophore of *s*-**1**. Thus, the rupture and formation of the intramolecular hydrogen bond would trigger a conformational transition, leading to the corresponding spectral changes in the same way as the Schiff base systems. Second, compared to the azomethine group, the amide linkage has a better tolerance to hydrolysis, which will endow the amide-type molecular switches with enhanced stability.

Figure 8 displays the CD and UV−vis titration spectra of *s*-**3** upon successive addition of TBAOH in DMSO. It can be seen

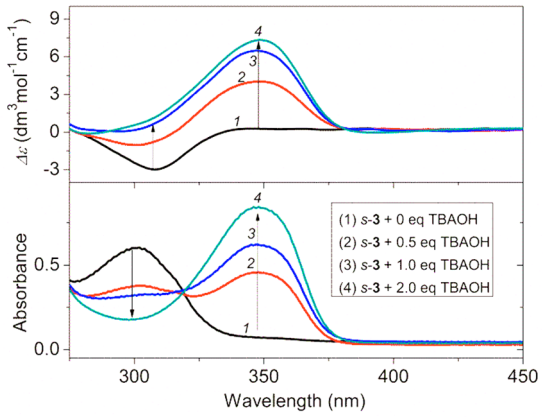

Figure 8. CD and UV−vis titration spectra of *s*-**3** (1×10^{-4} mol/L) in DMSO with increasing amount of TBAOH (0, 0.5, 1.0, and 2.0 equiv, respectively).

that free *s*-**3** displays a CD spectrum with a negative Cotton effect associated with the absorption near 309 nm. On addition of increasing amounts of TBAOH (0−2.0 equiv), the negative CD signal reduces gradually and finally turns into a new band with positive CE at 349 nm. The positive CD maximum is ∼1.8-fold more intensive than that of the original negative CE, which is different from *s*-**1**. As expected, for the amide system the base-induced CD change could also be totally reversed to the original state by acidification. Upon alternate addition of base and acid, such a reverse of CE signs can be repeated five times without a noticeable loss of signal intensities (Figure S1, Supporting Information), which is nearly the same as that observed in the case of *s*-**1**.

Also noteworthy is that the sense of Cotton effect in the CD spectrum of *s*-**3** changes from negative to positive upon deprotonation (Figure 8), whereas for *s*-**1** the CD band inverts from positive to negative (Figure 2). In spite of this, the sign of observed CEs in experimental CD spectra of *s*-**3** and its deprotonated species can be still predicted by using the simple conformational analysis and TDDFT computations as done above for *s*-**1**.

Geometry optimizations were conducted using the DFT method at the B3LYP/6-311++G**/IEFPCM(DMSO) level of theory, yielding the two most stable conformers (*s*-**3a**, *s*-**3b**) for *s*-**3** and one preferred conformer (*s*-**3c**) over all possible *s*-**3**$^-$ isomers (Figure 9). For *s*-**3a** and *s*-**3b**, the former has a relative

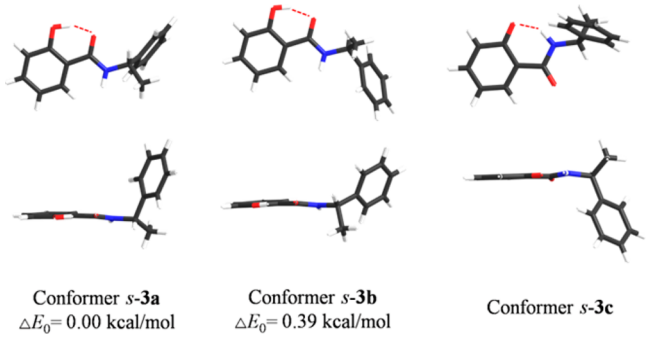

Figure 9. Optimized structures of the most stable conformers *s*-**3a** and *s*-**3b** for *s*-**3** and *s*-**3c** for *s*-**3**$^-$, obtained at the B3LYP/6-311++G**/IEFPCM(DMSO) level of theory (with relative energies). Each conformer is shown as a side (above) and top (below) view, in which oxygen and nitrogen atoms are red and blue, respectively, and intramolecular hydrogen bonds are represented asred dotted lines.

energy of 0.39 kcal/mol with a population of 65.49%, whereas the latter accounts for 34.07% of the population. Apparently, these conformers are stabilized by the intramolecular hydrogen-bonding interactions, where the amide group behaves as a hydrogen-bond acceptor in *s*-**3** and as a hydrogen-bond donor in *s*-**3**$^-$. Upon deprotonation of *s*-**3**, the original hydrogen bond breaks to form a new internal hydrogen bond between the amide N−H and phenolate oxyanion in the deprotonated species. Such a rearrangement of the intramolecular hydrogen bonding induced by the deprotonation of phenolic hydroxyl has been fully demonstrated in the previous reports on achiral salicylamide derivatives.[96−100]

To assess the reliability of theoretical ECD spectra, we performed TDDFT computations at the B3LYP/6-311++G**/IEFPCM(DMSO) level of theory for the amide-type molecular switch and compared the results to experiment (Figure 10). It can be seen that the averaged theoretical ECD agrees reasonably well agree with the experimental spectra, although the B3LYP functional slightly underestimates the CE's positions of *s*-**3** and *s*-**3**$^-$ by 16 and 19 nm, respectively. Also, the sign of the CEs of the amide derivative is in accord with that predicted by the exciton chirality rule.[101] As depicted in Figure 11, the most important contributor *s*-**3a** makes a negative contribution to the CD band of *s*-**3** whereas the contribution of the dominant conformer *s*-**3c** is positive for *s*-**3**$^-$. Accordingly, the reversible chiroptical switching behavior of the acid/base-induced amide-type molecular switch may be regarded as the consequence of the conformational transition about the amide attachment bond driven by the hydrogen bonding reorganization (Figure 11).

CONCLUSION

In the present work, we demonstrated a new strategy to construct stimuli-responsive molecular switches that show a

dx.doi.org/10.1021/jp410370q | J. Phys. Chem. A 2014, 118, 283−292

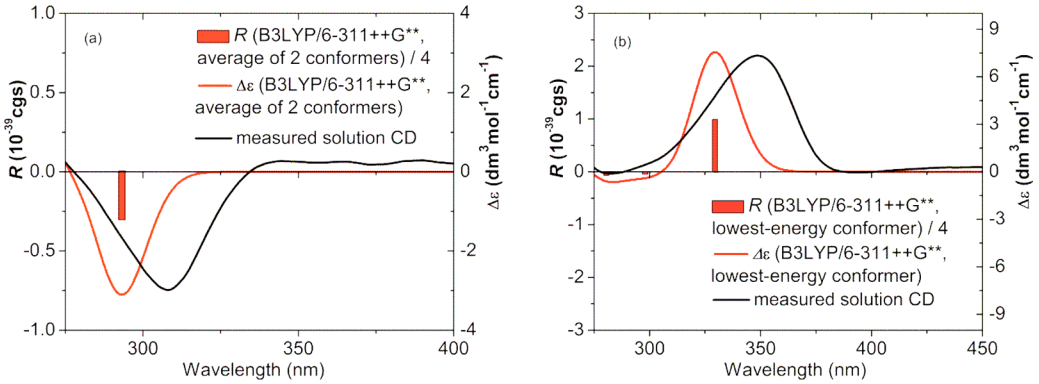

Figure 10. Experimental and Boltzmann-averaged ECD solution spectra of *s*-**3** (a) and *s*-**3**$^-$ (b) optimized by the B3LYP/6-311++G**/IEFPCM(DMSO) method. Vertical bars represent the rotational strengths *R* in 10^{-39} cgs units.

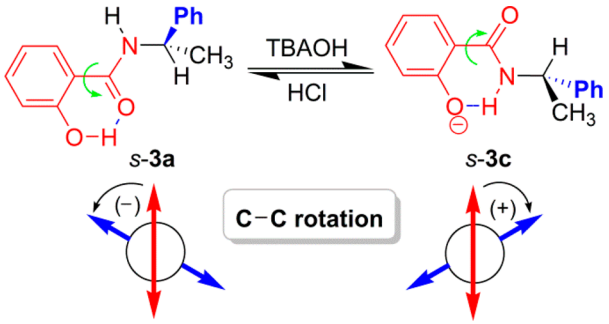

Figure 11. Prediction of CD signs for *s*-**3** and *s*-**3**$^-$ on the basis of their respective most stable conformations (*s*-**3a**, *s*-**3c**) obtained at the B3LYP/6-311++G**/IEFPCM(DMSO) level of theory. Each conformer has a particular chirality of coupling as shown.

reversible chiroptical inversion through the controlled C–C single bond rotation. The theoretical calculations provided useful insight into the conformational transition and intramolecular interaction and allow for elucidation of the observed chiroptical inversion behaviors. To the best of our knowledge, despite several examples of chiroptical inversion due to the single bond rotation,[74−76,102] no chiroptical molecular switches based on the proposed working mechanism have been reported until now. The feasibility of the approach has been successfully confirmed by simple chiral salicylaldehyde Schiff bases and a salicylamide analog. Compared to the existing molecule-based chiral inversion systems, this promising new type of chiroptical switching molecule is relatively unique as it does not involve any covalent bond formation/breakage and thus possesses distinct advantages, such as fast switching rate, high reversibility and fatigue resistance, and the nondestructive readout. Thus, such dynamic chiroptical inversion systems are expected to find potential applications in molecular recognition, chemosensors, or the construction of molecular-scale devices. More importantly, these findings suggest that the use of the conformational transition about a single bond may serve as the basis for designing chiroptical inversion systems.

Taking into account the straightforward preparation of the chiroptical molecular switches, as well as virtually unlimited structural flexibility provided by the modular nature of our finding, various chiral molecules containing imine or amide skeleton motif could be prepared and fine-tuned to control stability and rate of interconversion between the conformations having different chiroptical properties. Also, these modular structures make it possible to design a new generation of chiroptical molecular switches triggered by stimuli other than a change in pH, for instance, temperature, light, or electrochemical signals. Related work is now in progress.

EXPERIMENTAL SECTION

General Information. Compounds *s*-**2** and Me-*s*-**2** were prepared following the reported procedure.[17] All the solvents used were dried and distilled by usual procedures before use. Melting points were taken with a micro melting point apparatus and are uncorrected. ^{1}H and ^{13}C NMR spectra were recorded with tetramethylsilane as an internal standard and $CDCl_3$ as a solvent, respectively. UV–vis and CD spectra were obtained at 20 °C using a quartz cell of 1 cm. The optical rotation and ESI-MS were measured.

*Synthesis of (S)-N-Salicylidene-α-phenylethylamine (s-**1**).* To a solution of salicylaldehyde (1.22 g, 10.0 mmol) in ethanol (50 mL) was added (*S*)-α-phenylethylamine (1.21 g, 10.0 mmol). After 12 h of reflux, the solvent was removed under reduced pressure to give the crude product. The product was recrystallized from *n*-hexane to give a yellow solid in 83% yield (2.02 g). Mp: 73.6–74.3 °C. $[\alpha]_D^{20}$ = +121° (0.01 g/mL, DMSO). ^{1}H NMR (500 MHz, $CDCl_3$): δ 13.48 (bs, 1H), 8.22 (s, 1H), 7.20–7.40 (m, 7H), 6.96 (d, 1H), 6.86 (t, 1H), 4.53 (m, 1H), 1.63 (d, 3H). ^{13}C NMR (125 MHz, $CDCl_3$): δ 163.7, 161.3, 143.9, 132.5, 131.3, 128.9, 127.3, 126.5, 119.1, 118.8, 68.7, 25.2. MS (ESI, *m*/*z* ([M + H]$^+$)): calcd, 226.2; found, 226.1. (*R*)-*N*-Salicylidene-α-phenylethylamine (*r*-**1**) was prepared by the same method as that for *s*-**1** except for the use of (*R*)-α-phenylethylamine as the starting material.

*Synthesis of (S)-1-(1-Methylbenzyliminomethyl)-2-ethoxynaphthalene (Et-s-**2**).* Ethyl bromide (1.5 g, 13.9 mmol), 2-hydroxyl-1-naphthaldehyde (1.72 g, 10.0 mmol), and K_2CO_3 (5.0 g, 36.2 mmol) were mixed in dry acetone (50 mL) under a N_2 atmosphere. The resulting mixture was stirred at 40 °C for 36 h and then poured into a large amount of water to precipitate the etherated product (2-ethoxy-1-naphthaldehyde) as a white solid. The intermediate was recrystallized from *n*-hexane to give a colorless crystal (1.8 g, 91%).

The mixture of 2-ethoxy-1-naphthaldehyde (0.8 g, 4.0 mmol) and (*S*)-α-phenylethylamine (0.5 g, 4.2 mmol) in ethanol (50 mL) was refluxed for 12 h. After removel of solvent, the resulting white solid was recrystallized from *n*-hexane to give the desired product as a colorless crystal (1.1 g, 83%). Mp: 60.2–60.7 °C. $[\alpha]_D^{20}$ = +85° (0.01g/mL, THF/*n*-hexane, v/v = 1:4). ^{1}H NMR (400 MHz, $CDCl_3$): δ 9.32 (d, 1H), 9.20 (s, 1H), 7.88 (d, 1H), 7.76 (d, 1H), 7.51–7.60 (m, 3H), 7.35–

dx.doi.org/10.1021/jp410370q | J. Phys. Chem. A 2014, 118, 283–292

7.42 (m, 3H), 7.24−7.31 (m, 2H), 4.62−4.67 (m, 1H), 4.20−4.26 (m, 2H), 1.71 (d, 3H), 1.48 (t, 3H). ^{13}C NMR (125 MHz, $CDCl_3$): δ 157.4, 145.7, 132.2, 129.2, 128.3, 127.9, 127.7, 126.7, 126.6, 125.8, 123.9, 117.9, 114.1, 71.6, 65.3, 25.5, 15.0. MS (ESI, m/z ($[M + H]^+$)): calcd, 304.1; found, 304.4.

Synthesis of N-(S)-1-Phenylethyl-2-hydroxybenzamide (s-3). Methyl salicylate (1.52 g, 10.0 mmol) and (*S*)-α-phenylethylamine (1.50 g, 12.4 mmol) were mixed and heated at 100 °C for 20 h. The reaction mixture was cooled to room temperature and the resulteing product was recrystallized from *n*-hexane and ethyl acetate to give a white crystal (1.51 g, 62%). Mp: 108.5−109.4 °C. $[\alpha]_D^{20}$ = +15° (0.01 g/mL, DMSO). ^{1}H NMR (400 MHz, $CDCl_3$): δ 12.29 (s, 1H), 7.47−7.28 (m, 7H), 6.98 (d, 1H), 6.88 (t, 1H), 6.47 (b, 1H), 5.31 (m, 1H), 1.64 (d, 3H). ^{13}C NMR (100 MHz, $CDCl_3$): δ 169.1, 161.5, 142.4, 134.2, 128.8, 127.6, 126.1, 125.3, 118.6, 114.1, 49.0, 21.7. MS (ESI, m/z ($[M + H]^+$)): calcd, 242.1; found, 242.2.

Computations. Geometry optimizations and zero-point energies of the compounds were performed by TDDFT calculations at the B3LYP level[103,104] with a 6-311++G** basis set using "Gaussian03 program".[105] Vibration frequencies were used to confirm intermediates (number of imaginary frequencies = 0). This DFT calculation was proved economic and reliable in our previous work.[106,107]

■ ASSOCIATED CONTENT

Supporting Information

Switchable behavior illustration, selected CD, UV−vis, and ECD titration spectra, stick conformations, the optical rotation values for *s*-**1** and *s*-**3** before and after addition of TBAOH, and NMR and ESI−MS spectra of compounds. This information is available free of charge via the Internet at http://pubs.acs.org.

■ AUTHOR INFORMATION

Corresponding Authors

*L. Jiang: e-mail, cejlm@zju.edu.cn.
*J. Ling: e-mail, lingjun@zju.edu.cn.

Notes

The authors declare no competing financial interest.

■ ACKNOWLEDGMENTS

The authors are indebted to the financial support by the National Natural Science Foundation of China (Grant No. 21074107).

■ REFERENCES

(1) Miyake, H.; Tsukube, H. Coordination Chemistry Strategies for Dynamic Helicates: Time-Programmable Chirality Switching with Labile and Inert Metal Helicates. *Chem. Soc. Rev.* **2012**, *41*, 6977−6991.
(2) Song, G. T.; Ren, J. S. Recognition and Regulation of Unique Nucleic Acid Structures by Small Molecules. *Chem. Commun.* **2010**, *46*, 7283−7294.
(3) Maeda, K.; Mochizuki, H.; Watanabe, M.; Yashima, E. Switching of Macromolecular Helicity of Optically Active Poly(phenylacetylene)s Bearing Cyclodextrin Pendants Induced by Various External Stimuli. *J. Am. Chem. Soc.* **2006**, *128*, 7639−7650.
(4) Canary, J. W.; Mortezaei, S.; Liang, J. A. Redox-Reconfigurable Tripodal Coordination Complexes: Stereodynamic Molecular Switches. *Chem. Commun.* **2010**, *46*, 5850−5860.
(5) Feringa, B. L.; van Delden, R. A.; Koumura, N.; Geertsema, E. M. Chiroptical Molecular Switches. *Chem. Rev.* **2000**, *100*, 1789−1816.
(6) Fujiki, M. Switching Handedness in Optically Active Polysilanes. *J. Organomet. Chem.* **2003**, *685*, 15−34.
(7) Guo, P. Z.; Liu, M. H.; Zhao, X. S. Studies of Chiroptical Switch. *Prog. Chem.* **2008**, *20*, 644−649.
(8) Liu, W. J.; Cao, D. R. Progress in Molecular Chiroptical Switches. *Chinese J. Org. Chem.* **2008**, *28*, 1336−1347.
(9) Soloshonok, V. A.; Ueki, H.; Moore, J. L.; Ellis, T. K. Design and Synthesis of Molecules with Switchable Chirality via Formation and Cleavage of Metal-Ligand Coordination Bonds. *J. Am. Chem. Soc.* **2007**, *129*, 3512−3513.
(10) Fenniri, H.; Deng, B. L.; Ribbe, A. E. Helical Rosette Nanotubes with Tunable Chiroptical Properties. *J. Am. Chem. Soc.* **2002**, *124*, 11064−11072.
(11) Johnson, R. S.; Yamazaki, T.; Kovalenko, A.; Fenniri, H. Molecular Basis for Water−Promoted Supramolecular Chirality Inversion in Helical Rosette Nanotubes. *J. Am. Chem. Soc.* **2007**, *129*, 5735−5743.
(12) Lohr, A.; Lysetska, M.; Wurthner, F. Supramolecular Stereomutation in Kinetic and Thermodynamic Self-Assembly of Helical Merocyanine Dye Nanorods. *Angew. Chem., Int. Ed.* **2005**, *44*, 5071−5074.
(13) Palmans, A. R. A.; Meijer, E. W. Amplification of Vhirality in Dynamic Supramolecular Aggregates. *Angew. Chem., Int. Ed.* **2007**, *46*, 8948−8968.
(14) Zhang, L.; Liu, M. H. Supramolecular Chirality and Chiral Inversion of Tetraphenylsulfonato Porphyrin Assemblies on Optically Active Polylysine. *J. Phys. Chem. B* **2009**, *113*, 14015−14020.
(15) Abe, H.; Masuda, N.; Waki, M.; Inouye, M. Regulation of Saccharide Binding with Basic Poly(ethynylpyridine)s by H^+-induced Helix Formation. *J. Am. Chem. Soc.* **2005**, *127*, 16189−16196.
(16) Cheuk, K. K. L.; Lam, J. W. Y.; Lai, L. M.; Dong, Y. P.; Tang, B. Z. Syntheses, Hydrogen−Bonding Interactions, Tunable Chain Helicities, and Cooperative Supramolecular Associations and Dissociations of Poly(phenylacetylene)s Bearing L-Valine Pendants: Toward the Development of Proteomimetic Polyenes. *Macromolecules* **2003**, *36*, 9752−9762.
(17) Fujiki, M.; Koe, J. R.; Motonaga, M.; Nakashima, H.; Terao, K.; Teramoto, A. Computing Handedness: Quantized and Superposed Switch and Dynamic Memory of Helical Polysilylene. *J. Am. Chem. Soc.* **2001**, *123*, 6253−6261.
(18) Inouye, M.; Waki, M.; Abe, H. Saccharide−Dependent Induction of Chiral Helicity in Achiral Synthetic Hydrogen−Bonding Oligomers. *J. Am. Chem. Soc.* **2004**, *126*, 2022−2027.
(19) Langeveld-Voss, B. M. W.; Christiaans, M. P. T.; Janssen, R. A. J.; Meijer, E. W. Inversion of Optical Activity of Chiral Polythiophene Aggregates by a Change of Solvent. *Macromolecules* **1998**, *31*, 6702−6704.
(20) Maeda, K.; Morino, K.; Okamoto, Y.; Sato, T.; Yashima, E. Mechanism of Helix Induction on a Stereoregular Poly((4-carboxyphenyl)acetylene) with Chiral Amines and Memory of the Macromolecular Helicity Assisted by Interaction with Achiral Amines. *J. Am. Chem. Soc.* **2004**, *126*, 4329−4342.
(21) Maeda, K.; Yashima, E. Dynamic Helical Structures: Detection and Amplification of Chirality. *Supramolecular Chirality* **2006**, *265*, 47−88.
(22) Nakashima, H.; Fujiki, M.; Koe, J. R.; Motonaga, M. Solvent and Temperature Effects on the Chiral Aggregation of Poly(alkylarylsilane)s Bearing Remote Chiral Groups. *J. Am. Chem. Soc.* **2001**, *123*, 1963−1969.
(23) Nakashima, H.; Koe, J. R.; Torimitsu, K.; Fujiki, M. Transfer and Amplification of Chiral Molecular Information to Polysilylene Aggregates. *J. Am. Chem. Soc.* **2001**, *123*, 4847−4848.
(24) Nonokawa, R.; Yashima, E. Detection and Amplification of a Small Enantiomeric Imbalance in α-Amino Acids by a Helical Poly(phenylacetylene) with Crown Ether Pendants. *J. Am. Chem. Soc.* **2003**, *125*, 1278−1283.
(25) Pijper, D.; Feringa, B. L. Molecular Transmission: Controlling the Twist Sense of a Helical Polymer with a Single Light−Driven Molecular Motor. *Angew. Chem., Int. Ed.* **2007**, *46*, 3693−3696.
(26) Pijper, D.; Jongejan, M. G. M.; Meetsmia, A.; Feringa, B. L. Light-Controlled Supramolecular Helicity of a Liquid Crystalline

Phase Using a Helical Polymer Functionalized with a Single Chiroptical Molecular Switch. *J. Am. Chem. Soc.* **2008**, *130*, 4541−4552.
(27) Sakurai, S. I.; Okoshi, K.; Kumaki, J.; Yashima, E. Two-Dimensional Surface Chirality Control by Solvent-Induced Helicity Inversion of a Helical Polyacetylene on Graphite. *J. Am. Chem. Soc.* **2006**, *128*, 5650−5651.
(28) Satrijo, A.; Meskers, S. C. J.; Swager, T. M. Probing a Conjugated Polymer's Transfer of Organization-Dependent Properties from Solutions to Films. *J. Am. Chem. Soc.* **2006**, *128*, 9030−9031.
(29) Tang, H. Z.; Boyle, P. D.; Novak, B. M. Chiroptical Switching Polyguanidine Synthesized by Helix-Sense-Selective Polymerization Using [(*R*)-3,3′-dibromo-2,2′-binaphthoxy](di-tert-butoxy)titanium (IV) Catalyst. *J. Am. Chem. Soc.* **2005**, *127*, 2136−2142.
(30) Waki, M.; Abe, H.; Inouye, M. Translation of Mutarotation into Induced Circular Dichroism Signals through Helix Inversion of Host Polymers. *Angew. Chem., Int. Ed.* **2007**, *46*, 3059−3061.
(31) Yashima, E.; Maeda, K. Chirality-Responsive Helical Polymers. *Macromolecules* **2008**, *41*, 3−12.
(32) Yashima, E.; Maeda, K.; Nishimura, T. Detection and Amplification of Chirality by Helical Polymers. *Chem−Eur. J.* **2004**, *10*, 42−51.
(33) Yashima, E.; Maeda, K.; Sato, O. Switching of a Macromolecular Helicity for Visual Distinction of Molecular Recognition Events. *J. Am. Chem. Soc.* **2001**, *123*, 8159−8160.
(34) Yashima, E.; Maeda, Y.; Okamoto, Y. Helix-Helix Transition of Optically Active Poly((1*R*,2*S*)-*N*-(4-ethynylbenzyl)norephedrine) Induced by Diastereomeric Acid-Base Complexation Using Chiral Stimuli. *J. Am. Chem. Soc.* **1998**, *120*, 8895−8896.
(35) Yashima, E.; Matsushima, T.; Okamoto, Y. Chirality Assignment of Amines and Amino Alcohols Based on Circular Dichroism Induced by Helix Formation of a Stereoregular Poly((4-carboxyphenyl)-acetylene) through Acid-Base Complexation. *J. Am. Chem. Soc.* **1997**, *119*, 6345−6359.
(36) Dolain, C.; Jiang, H.; Leger, J. M.; Guionneau, P.; Huc, I. Chiral Induction in Quinoline-Derived Oligoamide Foldamers: Assignment of Helical Handedness and Role of Steric Effects. *J. Am. Chem. Soc.* **2005**, *127*, 12943−12951.
(37) Dolain, C.; Leger, J. M.; Delsuc, N.; Gornitzka, H.; Huc, I. Probing Helix Propensity of Monomers within a Helical Oligomer. *P Natl. Acad. Sci. U. S. A.* **2005**, *102*, 16146−16151.
(38) Hou, J. L.; Yi, H. P.; Shao, X. B.; Li, C.; Wu, Z. Q.; Jiang, X. K.; Wu, L. Z.; Tung, C. H.; Li, Z. T. Helicity Induction in Hydrogen-Bonding-Driven Zinc Porphyrin Foldamers by Chiral C_{60}-Incorporating Histidines. *Angew. Chem., Int. Ed.* **2006**, *45*, 796−800.
(39) Ikeda, C.; Yoon, Z. S.; Park, M.; Inoue, H.; Kim, D.; Osuka, A. Helicity Induction and Two-Photon Absorbance Enhancement in Zinc(II) Meso-Meso Linked Porphyrin Oligomers via Intermolecular Hydrogen Bonding Interactions. *J. Am. Chem. Soc.* **2005**, *127*, 534−535.
(40) Inai, Y.; Ousaka, N.; Okabe, T. Mechanism for the Noncovalent Chiral Domino Effect: New Paradigm for the Chiral Role of the *N*-Terminal Segment in a 3_{10}-Helix. *J. Am. Chem. Soc.* **2003**, *125*, 8151−8162.
(41) Inai, Y.; Tagawa, K.; Takasu, A.; Hirabayashi, T.; Oshikawa, T.; Yamashita, M. Induction of One-Handed Helical Screw Sense in Achiral Peptide through the Domino Effect Based on Interacting Its *N*-Terminal Amino Group with Chiral Carboxylic Acid. *J. Am. Chem. Soc.* **2000**, *122*, 11731−11732.
(42) Jiang, H.; Dolain, C.; Leger, J. M.; Gornitzka, H.; Huc, I. Switching of Chiral Induction in Helical Aromatic Oligoamides Using Solid State-Solution State Equilibrium. *J. Am. Chem. Soc.* **2004**, *126*, 1034−1035.
(43) Maurizot, V.; Dolain, C.; Huc, I. Intramolecular versus Intermolecular Induction of Helical Handedness in Pyridinedicarboxamide Oligomers. *Eur. J. Org. Chem.* **2005**, *7*, 1293−1301.
(44) Meudtner, R. M.; Hecht, S. Helicity Inversion in Responsive Foldamers Induced by Achiral Halide Ion Guests. *Angew. Chem., Int. Ed.* **2008**, *47*, 4926−4930.
(45) Prince, R. B.; Barnes, S. A.; Moore, J. S. Foldamer-Based Molecular Recognition. *J. Am. Chem. Soc.* **2000**, *122*, 2758−2762.
(46) Suk, J. M.; Naidu, V. R.; Liu, X. F.; Lah, M. S.; Jeonet, K. S. A Foldamer-Based Chiroptical Molecular Switch That Displays Complete Inversion of the Helical Sense upon Anion Binding. *J. Am. Chem. Soc.* **2011**, *133*, 13938−13941.
(47) Barcena, H. S.; Holmes, A. E.; Zahn, S.; Canary, J. W. Redox Inversion of Helicity in Propeller-Shaped Molecules Derived from *S*-Methyl Cysteine and Methioninol. *Org. Lett.* **2003**, *5*, 709−711.
(48) Barcena, H. S.; Liu, B.; Mirkin, M. V.; Canary, J. W. An Electrochiroptical Molecular Switch: Mechanistic and Kinetic Studies. *Inorg. Chem.* **2005**, *44*, 7652−7660.
(49) Biscarini, P.; Kuroda, R. Stereoselective Synthesis and Characterization of the Optically Labile Chiral Cr(III) Complex Δ-$(+)_{589}\{Cr[(-)bdtp]_3\}$. *Inorg. Chim. Acta* **1988**, *154*, 209−214.
(50) Chambers, J. A.; Gillard, R. D.; Williams, P. A.; Vagg, R. S. Chiral Metal-Complexes. 8. Chiroptical and 1H-NMR Studies on Diastereoisomeric Ternary Complexes Of Co(III) with 1,10-Phenanthroline and R,R-Tartaric Acid or S-Malic Acid. *Inorg. Chim. Acta* **1983**, *72*, 263−268.
(51) Gregolinski, J.; Slepokura, K.; Lisowski, J. Lanthanide Complexes of the Chiral Hexaaza macrocycle and Its Meso-Type Isomer: Solvent-Controlled Helicity Inversion. *Inorg. Chem.* **2007**, *46*, 7923−7934.
(52) Hiraoka, S.; Harano, K.; Tanaka, T.; Shiro, M.; Shionoya, M. Quantitative Formation of Sandwich-Shaped Trinuclear Silver(I) Complexes and Dynamic Nature of Their $P \rightleftharpoons M$ Flip Motion in Solution. *Angew. Chem., Int. Ed.* **2003**, *42*, 5182−5185.
(53) Hutin, M.; Nitschke, J. Solvent-Tunable Inversion of Chirality Transfer from Carbon to Copper. *Chem. Commun.* **2006**, *16*, 1724−1726.
(54) Kita, M.; Yamanari, K. The Effect of Counter Cations on Second-Order Asymmetric Transformations in *fac*-Δ- and Λ-tris(*R*-cysteinato-*N*,*S*)cobaltate(III) Complexes and the Kinetics of Mutarotation. *J. Chem. Soc., Dalton* **1999**, *8*, 1221−1226.
(55) Lin, R.; Zhang, H.; Li, S. H.; Chen, L. Q.; Zhang, W. G.; Wen, T. B.; Zhang, H.; Xia, H. P. pH-Switchable Inversion of the Metal-Centered Chirality of Metallabenzenes: Opposite Stereodynamics in Reactions of Ruthenabenzene with *L*- and *D*-Cysteine. *Chem.—Eur. J.* **2011**, *17*, 2420−2427.
(56) Martinez, A.; Guy, L.; Dutasta, J. P. Reversible, Solvent-Induced Chirality Switch in Atrane Structure: Control of the Unidirectional Motion of the Molecular Propeller. *J. Am. Chem. Soc.* **2010**, *132*, 16733−16734.
(57) Misaki, H.; Miyake, H.; Shinoda, S.; Tsukube, H. Asymmetric Twisting and Chirality Probing Properties of Quadruple-Stranded Helicates: Coordination Versatility and Chirality Response of Na^+, Ca^{2+}, and La^{3+} Complexes with Octadentate Cyclen Ligand. *Inorg. Chem.* **2009**, *48*, 11921−11928.
(58) Miyake, H.; Hikita, M.; Itazaki, M.; Nakazawa, H.; Sugimoto, H.; Tsukube, H. A Chemical Device that Exhibits Dual Mode Motions: Dynamic Coupling of Amide Coordination Isomerism and Metal-Centered Helicity Inversion in a Chiral Cobalt(II) Complex. *Chem.—Eur. J.* **2008**, *14*, 5393−5396.
(59) Miyake, H.; Sugimoto, H.; Tamiaki, H.; Tsukube, H. Dynamic Helicity Inversion in an Octahedral Cobalt(II) Complex System via Solvato-Diastereomerism. *Chem. Commun.* **2005**, *34*, 4291−4293.
(60) Miyake, H.; Ueda, M.; Murota, S.; Sugimoto, H.; Tsukube, H. Helicity Inversion from Left- to Right-Handed Square Planar Pd(II) Complexes: Synthesis of a Diastereomer Pair from a Single Chiral Ligand and Their Structure Dynamism. *Chem. Commun.* **2012**, *48*, 3721−3723.
(61) Miyake, H.; Yoshida, K.; Sugimoto, H.; Tsukube, H. Dynamic Helicity Inversion by Achiral Anion Stimulus in Synthetic Labile Cobalt(II) Complex. *J. Am. Chem. Soc.* **2004**, *126*, 6524−6525.
(62) Montgomery, C. P.; New, E. J.; Parker, D.; Peacock, R. D. Enantioselective Regulation of a Metal Complex in Reversible Binding to Serum Albumin: Dynamic Helicity Inversion Signalled by Circularly Polarised Luminescence. *Chem. Commun.* **2008**, *36*, 4261−4263.

(63) Yano, S.; Nakagoshi, M.; Teratani, A.; Kato, M.; Onaka, T.; Iida, M.; Tanase, T.; Yamamoto, Y.; Uekusa, H.; Ohashi, Y. Chiral Inversion around a Seven-Coordinated Cobalt Center Induced by an Interaction between Sugars and Sulfate Anions. *Inorg. Chem.* **1997**, *36*, 4187−4194.
(64) Zahn, S.; Canary, J. W. Electron-Induced Inversion of Helical Chirality in Copper Complexes of *N,N*-dialkylmethionines. *Science* **2000**, *288* (5470), 1404−1407.
(65) Chen, W. C.; Lee, Y. W.; Chen, C. T. Diastereoselective, Synergistic Dual-Mode Optical Switch with Integrated Chirochromic Helicene and Photochromic Bis-azobenzene Moieties. *Org. Lett.* **2010**, *12*, 1472−1475.
(66) Feringa, B. L. The Art of Building Small: From Molecular Switches to Molecular Motors. *J. Org. Chem.* **2007**, *72*, 6635−6652.
(67) Feringa, B. L.; Jager, W. F.; Delange, B.; Meijer, E. W. Chiroptical Molecular Switch. *J. Am. Chem. Soc.* **1991**, *113*, 5468−5470.
(68) Jager, W. F.; Dejong, J. C.; Delange, B.; Huck, N. P. M.; Meetsma, A.; Feringa, B. L. A Highly Stereoselective Optical Switching Process-Based on Donor-Acceptor-Substituted Dissymmetric Alkenes. *Angew. Chem., Int. Ed.* **1995**, *34*, 348−350.
(69) Mammana, A.; Carroll, G. T.; Areephong, J.; Feringa, B. L. A Chiroptical Photoswitchable DNA Complex. *J. Phys. Chem. B* **2011**, *115*, 11581−11587.
(70) Nishida, J.; Suzuki, T.; Ohkita, M.; Tsuji, T. A Redox Switch Based on Dihydro[5]helicene: Drastic Chiroptical Response Induced by Reversible C−C Bond Making/Breaking upon Electron Transfer. *Angew. Chem., Int. Ed.* **2001**, *40*, 3251−3254.
(71) Okano, K.; Ogino, S.; Kawamoto, M.; Yamashita, T. Mass Migration on a Polymer Surface Caused by Photoinduced Molecular Rotation. *Chem. Commun.* **2011**, *47*, 11891−11893.
(72) Takaishi, K.; Muranaka, A.; Kawamoto, M.; Uchiyama, M. Photoinversion of Cisoid/Transoid Binaphthyls. *Org. Lett.* **2012**, *14*, 276−279.
(73) Tietze, L. F.; Dufert, A.; Lotz, F.; Solter, L.; Oum, K.; Lenzer, T.; Beck, T.; Herbst-lrmer, R. Synthesis of Chiroptical Molecular Switches by Pd-Catalyzed Domino Reactions. *J. Am. Chem. Soc.* **2009**, *131*, 17879−17884.
(74) Haberhauer, G. A Metal-Ion-Driven Supramolecular Chirality Pendulum. *Angew. Chem., Int. Ed.* **2010**, *49*, 9286−9289.
(75) Jiang, X.; Lim, Y. K.; Zhang, B. J.; Opsitnick, E. A.; Baik, M. H.; Lee, D. Dendritic Molecular Switch: Chiral Folding and Helicity Inversion. *J. Am. Chem. Soc.* **2008**, *130*, 16812−16822.
(76) Reichert, S.; Breit, B. Development of an Axial Chirality Switch. *Org. Lett.* **2007**, *9*, 899−902.
(77) Smith, H. E. The Salicylidenamino Chirality Rule − A Method for the Establishment of the Absolute-Configurations of Chiral Primary Amines by Circular-Dichroism. *Chem. Rev.* **1983**, *83*, 359−377.
(78) Smith, H. E.; Neergaard, J. R.; Burrows, E. P.; Chen, F. M. Optically-Active Amines. 16. Exciton Chirality Method Applied to Salicylidenimine Chromophore − Salicylidenimine Chirality Rule. *J. Am. Chem. Soc.* **1974**, *96*, 2908−2916.
(79) Kamienski, B.; Schilf, W.; Dziembowska, T.; Rozwadowski, Z.; Szady-Chelmieniecka, A. The ^{15}N and ^{13}C Solid State NMR Study of Intramolecular Hydrogen Bond in Some Schiff's Bases. *Solid State Nucl. Magn. Reson.* **2000**, *16*, 285−289.
(80) Salman, S. R.; Kamounah, F. S. Tautomerism in 1-Hydroxy-2-naphthaldehyde Schiff Bases: Calculation of Tautomeric Isomers Using Carbon-13 NMR. *Spectrosc. Int. J.* **2003**, *17*, 747−752.
(81) Abbate, S.; Lebon, F.; Longhi, G.; Boiadjiev, S. E.; Lightner, D. A. Vibrational and Electronic Circular Dichroism of Dimethyl Mesobilirubins-XIIIα. *J. Phys. Chem. B* **2012**, *116*, 5628−5636.
(82) Jastrzebska, I.; Gorecki, M.; Frelek, J.; Santillan, R.; Siergiejczyk, L.; Morzycki, J. W. Photoinduced Isomerization of 23-Oxosapogenins: Conformational Analysis and Spectroscopic Characterization of 22-Isosapogenins. *J. Org. Chem.* **2012**, *77*, 11257−11269.
(83) Li, X. J.; Hopmann, K. H.; Hudecova, J.; Isaksson, J.; Novotna, J.; Stensen, W.; Andrushchenko, V.; Urbanova, M.; Svendsen, J. S.; Bour, P.; Ruud, K. Determination of Absolute Configuration and Conformation of a Cyclic Dipeptide by NMR and Chiral Spectroscopic Methods. *J. Phys. Chem. A* **2013**, *117*, 1721−1736.
(84) Nakai, Y.; Mori, T.; Inoue, Y. Theoretical and Experimental Studies on Circular Dichroism of Carbo[n]helicenes. *J. Phys. Chem. A* **2012**, *116*, 7372−7385.
(85) Nakai, Y.; Mori, T.; Inoue, Y. Circular Dichroism of (Di)methyl- and Diaza[6]helicenes. A Combined Theoretical and Experimental Study. *J. Phys. Chem. A* **2013**, *117*, 83−93.
(86) Nakai, Y.; Mori, T.; Sato, K.; Inoue, Y. Theoretical and Experimental Studies of Circular Dichroism of Mono- and Diazonia[6]helicenes. *J. Phys. Chem. A* **2013**, *117*, 5082−5092.
(87) Oh, K. I.; Kim, W.; Joo, C.; Yoo, D. G.; Han, H.; Hwang, G. S.; Cho, M. Azido Gauche Effect on the Backbone Conformation of β-Azidoalanine Peptides. *J. Phys. Chem. B* **2010**, *114*, 13021−13029.
(88) Park, E. K.; Park, B. J.; Choi, J. H.; Choi, K. H.; Cho, M. H. Chirality Transfer Effects in Proline-Substituted Coumarin Compounds. *J. Phys. Chem. B* **2009**, *113*, 11301−11305.
(89) Pikulska, A.; Hopmann, K. H.; Bloino, J.; Pecul, M. Circular Dichroism and Optical Rotation of Lactamide and 2-Aminopropanol in Aqueous Solution. *J. Phys. Chem. B* **2013**, *117*, 5136−5147.
(90) Sang, Y. M.; Yan, L. K.; Ma, N. N.; Wang, J. P.; Su, Z. M. TDDFT Studies on the Determination of the Absolute Configurations and Chiroptical Properties of Strandberg-Type Polyoxometalates. *J. Phys. Chem. A* **2013**, *117*, 2492−2498.
(91) Sun, P.; Xu, D. X.; Mandl, A.; Kurtan, T.; Li, T. J.; Schulz, B.; Zhang, W. Structure, Absolute Configuration, and Conformational Study of 12-Membered Macrolides from the Fungus *Dendrodochium sp*. Associated with the Sea Cucumber *Holothuria nobilis* Selenka. *J. Org. Chem.* **2013**, *78*, 7030−7047.
(92) Jaworska, M.; Welniak, M.; Zieciak, J.; Kozakiewicz, A.; Wojtczak, A. Bidentate Schiff Bases Derived from (*S*)-α-Methylbenzylamine as Chiral Ligands in the Electronically Controlled Asymmetric Addition of Diethylzinc to Aldehydes. *Arkivoc* **2011**, 189−204.
(93) Berova, N.; Di Bari, L.; Pescitelli, G. Application of Electronic Circular Dichroism in Configurational and Conformational Analysis of Organic Compounds. *Chem. Soc. Rev.* **2007**, *36*, 914−931.
(94) Liu, B. B.; Lu, W.; Du, G. H.; Chen, D.; Ling, J.; Jiang, L. M.; Shen, Z. Q. Design of an Optically Active Polystyrene Bearing Imine Pendants and Its Acid/Base-Triggered Chiroptical Switch Property. *Acta Polym. Sin.* **2013**, *4*, 436−442.
(95) The conformers of Et-*s*-**2**, *s*-**2**, and *s*-**2**$^-$ in solution were optimized with the PCM model for DMSO or hexane at the B3LYP/6-311++G** level of theory. The results showed that their respective solution conformers of lowest energy in both the solvents are the same.
(96) Kanamori, D.; Okamura, T.; Yamamoto, H.; Shimizu, S.; Tsujimoto, Y.; Ueyama, N. Structures of the Small-Molecule Bcl-2 Inhibitor (BH3I-2) and Its Related Simple Model in Protonated and Deprotonated Forms. *Bull. Chem. Soc. Jpn.* **2004**, *77*, 2057−2064.
(97) Kanamori, D.; Okamura, T. A.; Yamamoto, H.; Ueyama, N. Linear-to-Turn Conformational Switching Induced by Deprotonation of Unsymmetrically Linked Phenolic Oligoamides. *Angew. Chem., Int. Ed.* **2005**, *44*, 969−972.
(98) Kondo, M. Nuclear Magnetic-Resonance Study of Several *o*-Disubstituted Benzenes. *Bull. Chem. Soc. Jpn.* **1972**, *45*, 2790−2793.
(99) Mock, W. L.; Chua, D. C. Y. Exceptional Active-Site H-Bonding In Enzymes - Significance of the Oxyanion Hole in the Serine Proteases from a Model Study. *J. Chem. Soc., Perkin Trans. 2* **1995**, *11*, 2069−2074.
(100) Steinwender, E.; Mikenda, W. O−H...O(S) Hydrogen-Bonds in 2-Hydroxy(thio)Benzamides. Survey of Spectroscopic and Structural Data. *Monatsh. Chem.* **1990**, *121*, 809−820.
(101) Tanatani, A.; Yokoyama, A.; Azumaya, I.; Takakura, Y.; Mitsui, C.; Shiro, M.; Uchiyama, M.; Muranaka, A.; Kobayashi, N.; Yokozawa, T. Helical Structures of *N*-Alkylated Poly(*p*-benzamide)s. *J. Am. Chem. Soc.* **2005**, *127*, 8553−8561.

(102) Di Bari, L.; Pescitelli, G.; Salvadori, P. Conformational Study of 2,2′-homosubstituted 1,1′-Binaphthyls by Means of UV and CD Spectroscopy. *J. Am. Chem. Soc.* **1999**, *121*, 7998−8004.
(103) Becke, A. D. Density-Functional Thermochemistry. 3. The Role of Exact Exchange. *J. Chem. Phys.* **1993**, *98*, 5648−5652.
(104) Lee, C. T.; Yang, W. T.; Parr, R. G. Development of the Colle-Salvetti Correlation-Energy Formula into a Functional of the Electron-Density. *Phys. Rev. B* **1988**, *37*, 785−789.
(105) Frisch, M. J.; Trucks, G. W.; Schlegel, H. B.; Cheeseman, J. R.; Montgomery, J. A., Jr.; Vreven, T.; Kudin, K. N.; Burant, J. C.; Millam, J. M.; Iyengar, S. S.; et al. *Gaussian 03*; Gaussian, Inc.: Wallingford, CT, 2004.
(106) Ling, J.; Dai, Y. B.; Zhu, Y. H.; Sun, W. L.; Shen, Z. Q. Ring-Opening Polymerization of 1-Methyltrimethylene Carbonate by Rare Earth Initiators. *J. Polym. Sci., Part A: Polym. Chem.* **2010**, *48*, 3807−3815.
(107) Ling, J.; Huang, Y. X. Understanding the Ring-Opening Reaction of alpha-Amino Acid *N*-Carboxyanhydride in an Amine-Mediated Living Polymerization: A DFT Study. *Macromol. Chem. Phys.* **2010**, *211*, 1708−1711.